HHS Public Access

Author manuscript

Gut. Author manuscript; available in PMC 2020 February 01.

Published in final edited form as:

Gut. 2019 February ; 68(2): 301–312. doi:10.1136/gutjnl-2018-315994.

Human *CPA1* mutation causes digestive enzyme misfolding and chronic pancreatitis in mice

Eszter Hegyi and **Miklós Sahin-Tóth***

Center for Exocrine Disorders, Department of Molecular and Cell Biology, Boston University Henry M. Goldman School of Dental Medicine, Boston, MA 02118

Abstract

OBJECTIVE.—Chronic pancreatitis is a progressive, relapsing inflammatory disorder of the pancreas, which often develops in the background of genetic susceptibility. Recently, loss-of-function mutations in *CPA1*, which encodes the digestive enzyme carboxypeptidase A1, were described in sporadic early-onset cases and in hereditary pancreatitis. Mutation-induced misfolding of CPA1 and associated endoplasmic reticulum (ER) stress was suggested as potential disease mechanism, however, *in vivo* evidence has been lacking. The objective of the present study was to create a mouse model that recapitulates features of *CPA1*−associated chronic pancreatitis.

DESIGN.—We knocked-in the most frequently occurring p.N256K human *CPA1* mutation to the mouse *Cpa1* locus. Mutant mice were characterized with respect to pancreas pathology and ER stress and compared to C57BL/6N and *CPA1 null* control mice.

RESULTS.—In the *CPA1 N256K* mutant mice we observed hallmarks of chronic pancreatitis that included progressive acinar cell atrophy, inflammatory cell infiltration, fibrosis and acinar-ductal metaplasia. In contrast, similarly to the C57BL/6N mice, the *CPA1 null* control strain exhibited no signs of pancreatic disease. Mutation p.N256K induced misfolding of mouse CPA1 and resulted in elevated expression of ER stress markers *Hspa5* (BiP) and *Ddit3* (CHOP) both in cell culture and mutant mice.

CONCLUSION.—The results offer categorical evidence that *CPA1* mutations elicit enzyme misfolding and cause chronic pancreatitis via an ER-stress related mechanism.

Keywords

chronic pancreatitis; genetic mutation; protein misfolding; endoplasmic reticulum stress; mouse model of disease

*Correspondence to: Miklós Sahin-Tóth, 72 East Concord Street, Evans-433; Boston, MA 02118; Tel: (617) 358-3790, miklos@bu.edu.

AUTHOR CONTRIBUTIONS:

MST conceived and directed the study. EH and MST designed the experiments. EH performed the experiments. EH and MST analyzed the data. EH and MST wrote the manuscript.

COMPETING INTERESTS:

MST is a consultant for Takeda Pharmaceuticals, Inc. EH declares no competing financial interests.

INTRODUCTION

The inflammatory disease continuum of the pancreas includes the clinical diagnoses of acute pancreatitis, recurrent acute pancreatitis and chronic pancreatitis.[1] Onset and progression of a single episode of acute pancreatitis towards chronic pancreatitis is often determined by underlying genetic risk factors associated with digestive proteases or their inhibitor. Mutations in *PRSS1* (cationic trypsinogen), *SPINK1* (serine protease inhibitor Kazal type 1), *CTRC* (chymotrypsin C) increase activation of trypsinogen to trypsin in the pancreas and thereby result in acinar cell damage and inflammation.[2] A protective mutation in *PRSS2* (anionic trypsinogen) and an inversion at the *CTRB1-CTRB2* (chymotrypsin B1–B2) locus also modify trypsin levels and pancreatitis risk.[3, 4] Importantly, genetic risk in chronic pancreatitis can be mediated by mechanisms that are unrelated to trypsin activity. Thus, a subset of *PRSS1* mutations has no impact on trypsin activity but causes enzyme misfolding and elicits endoplasmic reticulum (ER) stress in cell culture experiments.[5, 6] Similarly, *CPA1* (carboxypeptidase A1) mutations cause enzyme misfolding *in vitro*, resulting in diminished CPA1 secretion, intracellular retention and degradation, and associated ER stress.[7, 8] *CPA1* mutations that elicit misfolding are highly overrepresented in pediatric cases of chronic pancreatitis and may be associated with autosomal dominant hereditary pancreatitis, indicating that these risk factors have a strong, essentially disease-causing effect.[7, 9] While the *in vitro* observations support a pathogenic role for mutation-induced misfolding and ER stress; evidence from appropriate animal models has been lacking and the disease mechanism of *CPA1* mutations has remained hypothetical. The unavailability of animal models not only limited our understanding of the disease mechanism but also hindered pre-clinical testing of novel therapeutics. Here we addressed this knowledge gap by generating a novel knock-in mouse strain carrying the human *CPA1* mutation p.N256K in the mouse *Cpa1* locus.

METHODS

Accession numbers.

NC_000072.6, *Mus musculus* strain C57BL/6J chromosome 6, GRCm38.p2 C57BL/6J; NM_025350.3, *Mus musculus* carboxypeptidase A1 (Cpa1) mRNA.

Generation of the *CPA1 N256K* and *CPA1 null* mouse strains.

Mice were on the C57BL/6N genetic background. The human *CPA1* mutation p.N256K was knocked-in to the mouse *Cpa1* locus using homologous recombination in C57BL/6 embryonic stem (ES) cells (Cyagen, Santa Clara, CA). The mouse *Cpa1* gene is located on chromosome 6; it spans ~8.5 kb and comprises 10 exons. The targeting vector contained the mouse *Cpa1* gene with the p.N256K mutation in exon 7 and a 1,941 nt sequence including a neomycin resistance gene flanked by loxP sites in intron 6, which served as a positive selection marker (Supplementary Fig S1). Correctly targeted ES cell clones were identified by long range PCR followed by Southern blot verification. Mutant ES cells were injected into mouse embryos (blastocysts), which were implanted into pseudopregnant females. The resulting chimeras were bred with wild-type C57BL/6N mice to achieve germline transmission of the mutant allele. This allele was designated as *CPA1 null*, because the

presence of the neomycin cassette resulted in diminished *Cpa1* mRNA and CPA1 protein expression. To remove the neomycin resistance gene, the mutant mice harboring the *CPA1 null* allele were bred with a Cre-deleter strain that expresses the Cre recombinase in the early mouse embryo (B6.FVB-Tg(EIIa-cre)C5379Lmgd/J; Jackson Laboratories). The final *CPA1 N256K* knock-in allele carried the p.N256K mutation in exon 7 and a 144 nt residual sequence in intron 6 containing a single loxP site (Supplementary Fig S2). C57BL/6N control mice were obtained from Charles River Laboratories (Wilmington, MA) or produced in our breeding facility from the same stock. *CPA1 N256K* and *CPA1 null* mice were maintained in homozygous state. Both male and female animals were studied.

Genotyping.

To genotype *CPA1 N256K* mice, we used primers that amplified exon 7 with parts of the flanking introns. The amplicon size from the wild-type allele was 646 bp, whereas the mutant allele yielded a 790 bp product due to the presence of the residual sequence in intron 6 (Supplementary Fig S2). The primer sequences were as follows. CPA1 N256K F1: 5'-AGT GGG ATG TAC CTT TGA GC-3'; CPA1 N256K R1: 5'-AGG CCC AAG TCC CTG AGT GT-3'. *CPA1 null* mice were first genotyped for the presence of the neomycin resistance gene using the CPA1 Neo F1 (5'-GAG CTT GCG GAA CCC TTA AT-3') and CPA1 N256K R1 primers. Positive mice yielded a 606 bp amplicon. Homozygosity was then verified by direct sequencing of the site of the p.N256K mutation after PCR amplification with the CPA1 N256K F2 (5'-TGA AGG TGT TGA TAG GTT ACT AG-3') and CPA1 N256K R1 primers which yielded a 509 bp product (Supplementary Fig S1).

All other experimental procedures are described in the online *Supplementary Methods* file.

RESULTS

Mutation-induced CPA1 misfolding and ER stress in cell culture.

The aim of this study was to generate a novel knock-in mouse strain harboring the most frequently found human *CPA1* mutation p.N256K in the native mouse *Cpa1* gene. To demonstrate feasibility of this approach, first we had to confirm that the p.N256K mutation in the context of mouse CPA1 induces misfolding and ER stress in the same manner as it was described for human CPA1. Therefore, we measured CPA1 secretion and ER stress markers in HEK 293T cells transfected with wild-type and mutant CPA1 expression plasmids. We found that the p.N256K CPA1 mutant was not secreted into the conditioned medium (Fig 1A,B), but was retained intracellularly (Fig 1B) and induced ER stress, as judged by increased *XBP1* splicing, and elevated mRNA levels for the ER chaperone *HSPA5* (BiP) and ER-stress associated pro-apoptotic transcription factor *DDIT3* (CHOP) (Fig 1C). These results indicate that we can successfully model the effects of human *CPA1* mutation p.N256K in mouse *Cpa1*.

Generation of the *CPA1 N256K* knock-in mouse strain.

A targeting vector containing the mouse *Cpa1* gene with the p.N256K mutation in exon 7 and a neomycin resistance cassette flanked by loxP sites in intron 6 was used to introduce the mutation into the mouse genome by homologous recombination in C57BL/6 embryonic

stem cells (Fig 2A). Mice carrying this targeted allele expressed diminished levels of *Cpa1* mRNA (Fig 2B) and CPA1 protein (Fig 2C) and were, therefore, designated as a *CPA1 null* strain and used as an additional control for our experiments. This control was important to distinguish between the effects due to loss of CPA1 protein/activity or to CPA1 misfolding. To obtain *CPA1 N256K* mutant mice, the neomycin cassette was excised by breeding with a Cre-deleter strain. The final *CPA1 N256K* strain harbored the p.N256K mutation in exon 7 and a residual loxP site in the neighboring intron. Although human *CPA1* mutations are found in the heterozygous state, in our experiments we used homozygous mice, which exhibited more robust and earlier changes in pathology.

CPA1 expression studies.

To characterize *Cpa1* mRNA expression in the pancreas of *CPA1 N256K* and *CPA1 null* strains, we prepared pancreatic cDNA from 1-month-old animals (Fig 2B). Analysis with qPCR revealed that in the *CPA1 N256K* strain *Cpa1* mRNA expression was reduced by 30%, relative to C57BL/6N controls, while in the *CPA1 null* strain it was diminished by 95%. The slight decrease in mRNA expression in the *CPA1 N256K* animals was likely due to the negative impact of the remaining single loxP site in intron 6. Western blot analysis of pancreatic homogenates from 1-month-old *CPA1 N256K* mice demonstrated reduced but still significant CPA1 protein content, compared to C57BL/6N control mice (Fig 2C). As expected, we did not detect CPA1 protein expression in the pancreas of *CPA1 null* mice (Fig 2C).

We isolated pancreatic acini from 6-week-old *CPA1 N256K* and C57BL/6N control mice and measured spontaneous and cerulein-induced CPA1 secretion to the culture medium (Fig 3). Relative to the wild-type CPA1 protein, secretion of the CPA1 p.N256K mutant was hardly detectable (Fig 3A). In contrast, western blot analysis of acinar cell lysates revealed high levels of mutant CPA1 protein, indicating intracellular retention. As seen with pancreas homogenates (cf Fig 2C), intracellular levels of the N256K mutant were somewhat reduced relative to the wild-type CPA1 content, indicating that some of the misfolded and retained mutant protein becomes degraded. We note that compared to cell culture experiments, degradation of mutant CPA1 protein is less efficient in mice.

Chronic pancreatitis in *CPA1 N256K* mice.

The two novel *CPA1* strains showed no apparent phenotypic alterations and bred normally. When followed up to 6 months, *CPA1 N256K* and *CPA1 null* mice gained weight with similar kinetics as the C57BL/6N controls (Fig 4A). Macroscopic pancreas morphology was comparable in *CPA1 null* and C57BL/6N control mice. In contrast, we observed smaller pancreata in *CPA1 N256K* mice starting at 3 months of age (not shown). Pancreas weight measurements confirmed atrophy in the *Cpa1 N256K* strain, which corresponded to ~35–40% decrease at 6 months of age (Fig 4B). To identify the histological changes underlying pancreatic atrophy in *CPA1 N256K* mice, we stained pancreas sections of 1, 3, 6 and 12 months old mice and compared these to the corresponding *CPA1 null* and C57BL/6N sections (Fig 5). Pancreas histology of *CPA1 null* mice was similar to C57BL/6N controls and showed no discernable changes over time. In contrast, we observed progressive pathological changes on sections from *CPA1 N256K* mice, which included loosely packed

tissue architecture due to loss of acini, infiltration of inflammatory cells and the presence of pseudotubular complexes (Fig 5A,B). Increased acinar cell vacuolization was also apparent at later time points. Quantification of the acinar cell area indicated ~30% loss by 12 months of age in *CPA1 N256K* mice (Fig 5C). The histological picture was consistent with the development of spontaneous, progressive chronic pancreatitis in mice carrying the homozygous *CPA1* p.N256K mutation. This conclusion was further corroborated by Masson's trichrome staining, which revealed widespread fibrotic changes among the remaining acini in *CPA1 N256K* mice (Fig 6A). Furthermore, pancreata from *CPA1 N256K* mice contained significantly higher hydroxyproline levels than those from *CPA1 null* or C57BL/6N control mice (Fig 6B). Acinar-ductal metaplasia (pseudotubular complexes) was also visualized by immunohistochemical staining for cytokeratin 19 and Sox9, which yielded strong positivity in *CPA1 N256K* sections (Fig 6C).

To evaluate possible ultrastructural changes in acinar cells from *CPA1 N256K* mice, we examined pancreas tissue by electron microscopy (Fig 7A) from 4-months-old mice. Zymogen granules showed comparable numbers and morphology in acinar cells from *CPA1 N256K* and C57BL/6N control mice. In *CPA1 N256K* mice, we observed some vacuolization and the presence of concentric arrangements of ER stacks (ER whorls) without visible ER dilations. Electron micrographs also showed pseudotubular complexes and macrophages between acini. Infiltration of macrophages was further confirmed by immunohistochemistry for the marker F4/80 in the pancreas of *CPA1 N256K* mice (Fig 7B).

Plasma amylase and intra-pancreatic trypsin in *CPA1 N256K* mice.

We examined blood levels of the pancreatitis marker amylase in *CPA1 N256K, CPA1 null* and C57BL/6N control mice at ages of 1 month, 3 months and 6 months. We detected a significant increase in plasma amylase in 1-month-old *CPA1 N256K* mice relative to the two other strains (Fig 8A). Consistent with subsequent acinar atrophy, no increase in plasma amylase was apparent at 3 and 6 months in *CPA1 N256K* mice. We also found a slight but significant decrease in plasma amylase in 1-month-old *CPA1 null* mice compared with C57BL/6N controls. This was likely due to the lower tissue content of amylase in *CPA1 null* mice at this age (not shown).

Intra-pancreatic trypsin activation was evaluated in pancreas homogenates from 1 month, 3 months and 6 months old mice. Remarkably, we observed significant elevations in trypsin activity in pancreata from *CPA1 N256K* mice relative to *CPA1 null* and C57BL/6N controls (Fig 8B). High trypsin activity persisted and even increased during the disease course.

ER stress in *CPA1 N256K* mice.

Finally, to determine whether the histological changes in the *CPA1 N256K* strain are associated with elevated ER stress markers, we measured pancreatic mRNA expression for the chaperone *Hspa5* (BiP) and the transcription factor *Ddit3* (CHOP) at 1 month (Fig 9A), 3 months (Fig 9B) and 12 months (Fig 9C) of age. Compared to C57BL/6N and *CPA1 null* controls, in *CPA1 N256K* mice BiP showed a consistent but modest upregulation, which was apparent as a trend at 1 month and 12 months but reached statistical significance at 3 months. In contrast, significant CHOP upregulation was observed in the pancreas of *CPA1*

N256K mice at all time points (Fig 9). We also measured *Hspa5* mRNA from isolated acinar cells of 6-week-old mice and found a 1.5-fold upregulation in cells from *CPA1 N256K* mice versus C57BL/6N controls (not shown). Finally, staining for markers of apoptosis (TUNEL, cleaved caspase 3) revealed very few positive cells at any given time tested (not shown); consistent with the relatively low levels of chronic ER stress observed and the slowly progressive nature of parenchymal atrophy.

DISCUSSION

Our thinking about the pathogenic mechanism of genetic risk factors in chronic pancreatitis has been shaped by biochemical and cell biological experiments while animal models have been conspicuously missing. This unique experimental trajectory of our field is partly to blame for the scarcity of novel therapeutic approaches, as the unavailability of pre-clinical models has hindered drug development. Genetic risk is mediated via two seemingly unrelated pathological pathways; the trypsin-dependent and the misfolding-dependent mechanisms.[2, 8] While the causative role of premature intra-pancreatic trypsin activation in pancreatitis onset has been appreciated for some time, the notion that mutation-induced misfolding may cause pancreatic pathology is relatively novel. The concept was first proposed in 2009, based on the observation that certain *PRSS1* mutations caused misfolding and ER stress in cell culture experiments.[5] More compelling evidence for ER-stress related pathogenesis came from our 2013 study that identified the association of loss-of-function variants in *CPA1* with early-onset chronic pancreatitis.[7] The majority of functionally defective *CPA1* variants exhibited the ‘misfolding phenotype’ of diminished secretion with intracellular retention and degradation. The most frequently found variant p.N256K was also shown to induce ER stress in AR42J rat acinar cells transfected with recombinant adenovirus. Recent studies demonstrating association of the p.L104P *PRSS1* variant and a novel p.S282P *CPA1* variant with autosomal dominant hereditary pancreatitis provided a convincing indication that misfolding variants can have strong, highly-penetrant genetic effects.[6, 9, 10] Importantly, both variants induced significant ER stress in cell culture, further corroborating the presumed link between misfolding, ER stress and chronic pancreatitis. However, despite the accumulation of highly suggestive evidence for the pathogenic role of the misfolding pathway, animal models that recapitulate *CPA1*−associated chronic pancreatitis, both phenotypically and mechanistically, remained a critical unmet challenge.

In the present study, we set out to address this problem by knocking in the most frequent human *CPA1* mutation p.N256K into the mouse *Cpa1* gene. First, we verified in cell culture experiments that the p.N256K mutation exerts the same effect on mouse CPA1 as it does on human CPA1. Indeed, the mutated mouse CPA1 exhibited the expected misfolding phenotype (diminished secretion, intracellular retention and degradation) and caused significant ER stress in cells, as judged by elevated BiP and CHOP mRNA levels and increased splicing of the *XBP1* mRNA. Next, the novel knock-in mouse strain was generated using a homologous recombination approach. To replicate the exact human situation, we created a constitutive *Cpa1* p.N256K allele expressed throughout the mouse’s life. In contrast to humans where *CPA1* mutations are heterozygous, we bred the mice to homozygosity to obtain stronger and earlier responses. It is important to note that

heterozygous mutant mice developed similar pancreatic lesions as homozygous animals but on a slower time-scale and to a smaller extent, which was impractical for experimental studies (not shown). In our study design, we also included a *CPA1 null* strain to demonstrate that the effects of the p.N256K mutation are not due to loss of CPA1 protein or activity.

Arguably, our most exciting finding is the progressive histological damage observed in the pancreas of *CPA1 N256K* mutant mice. Thus, starting at the age of 1 month, these animals exhibit classic signs of chronic pancreatitis including pancreatic atrophy due to loss of acini, fibrosis, tubular complexes (acinar-ductal metaplasia) and inflammatory cell infiltration. Approximately a third of the acinar parenchyma becomes ablated with no apparent change in islets. These observations clearly establish that the p.N256K mutation and, by extension, misfolding CPA1 variants in general, can directly cause chronic pancreatitis. Because no such changes were observed in the *CPA1 null* strain, the results also demonstrate that loss of CPA1 protein or activity *per se* are not harmful to the pancreas.

To examine whether the development of the progressive morphological changes were driven by mutation-induced misfolding, we investigated signs of ER stress in the *CPA1 N256K* strain. Interestingly, as revealed by electron microscopy, there were no apparent changes in ER morphology with the exception of a few ER whorls. Consistent with this picture, only a modest increase in the mRNA levels of the master chaperone BiP was observed. On the other hand, we found marked upregulation of the pro-apoptotic transcription factor CHOP. Taken together, the observations demonstrate that in *CPA1 N256K* mice chronic, relatively low-level ER stress results in CHOP-dependent acinar cell loss. In turn, acinar cell death triggers the other hallmarks of chronic pancreatitis such as inflammatory cell infiltration, fibrosis and acinar-to-ductal metaplasia.

An unexpected observation was the high trypsin activity present in the pancreata of the *CPA1 N256K* mice throughout the disease course. This finding raises the possibility that ER-stress somehow triggers trypsin-dependent pathological mechanisms and disease onset and progression may be ultimately driven by trypsin. Alternatively, high trypsin activity may be a marker of parenchymal damage rather than the cause of it.

Finally, it is important to highlight the potential pre-clinical utility of this new model of misfolding-induced chronic pancreatitis. The *CPA1 N256K* strain develops, gains weight and breeds normally. These properties together with the convenient time line of the development of the pancreatic lesions make this an ideal model to test the effects of various environmental insults (alcohol, smoking, high-fat diet) or pharmaceuticals on the progression of chronic pancreatitis.

In conclusion, we demonstrated that the human *CPA1* mutation p.N256K induces misfolding of mouse CPA1 and causes spontaneous and progressive chronic pancreatitis in the *CPA1 N256K* knock-in mouse, associated with the upregulation of the ER-stress related pro-apoptotic transcription factor CHOP. No pancreatic pathology was observed in *CPA1 null* mice, indicating that loss of CPA1 function *per se* does not lead to acinar cell damage. The observations offer convincing evidence for the pathogenic role of a misfolding-dependent

pathway in chronic pancreatitis and set the stage for interventions targeting ER-stress associated mechanisms in this disease.

Supplementary Material

Refer to Web version on PubMed Central for supplementary material.

ACKNOWLEDGEMENTS:

The authors are grateful to Andrea Geisz and Dorottya Berki for assistance with preliminary experiments.

FUNDING: This work was supported by the National Institutes of Health (NIH) grant R01 DK058088.

REFERENCES

1. Yadav D, Lowenfels AB. The epidemiology of pancreatitis and pancreatic cancer. Gastroenterology 2013, 144:1252–1261 [PubMed: 23622135]
2. Hegyi E, Sahin-Tóth M. Genetic risk in chronic pancreatitis: The trypsin-dependent pathway. Dig Dis Sci 2017, 62:1692–1701
3. Witt H, Sahin-Tóth M, Landt O, et al. A degradation-sensitive anionic trypsinogen (PRSS2) variant protects against chronic pancreatitis. Nat Genet 2006, 38:668–673 [PubMed: 16699518]
4. Rosendahl J, Kirsten H, Hegyi E, et al. Genome-wide association study identifies inversion in the *CTRB1-CTRB2* locus to modify risk for alcoholic and non-alcoholic chronic pancreatitis. Gut 2018 7 28; 67: 1855–1863. [Epub ahead of print] [PubMed: 28754779]
5. Kereszturi E, Szmola R, Kukor Z, et al. Hereditary pancreatitis caused by mutation-induced misfolding of human cationic trypsinogen: a novel disease mechanism. Hum Mutat 2009, 30:575–582 [PubMed: 19191323]
6. Balázs A, Hegyi P, Sahin-Tóth M. Pathogenic cellular role of the p.L104P human cationic trypsinogen variant in chronic pancreatitis. Am J Physiol Gastrointest Liver Physiol 2016, 310:G477–486 [PubMed: 26822915]
7. Witt H, Beer S, Rosendahl J, et al. Variants in *CPA1* are strongly associated with early onset chronic pancreatitis. Nat Genet 2013, 45:1216–1220 [PubMed: 23955596]
8. Sahin-Tóth M Genetic risk in chronic pancreatitis: the misfolding-dependent pathway. Curr Opin Gastroenterol 2017, 33:390–395 [PubMed: 28650851]
9. Kujko AA, Berki DM, Oracz G, et al. A novel p.Ser282Pro *CPA1* variant is associated with autosomal dominant hereditary pancreatitis. Gut 2017, 66:1728–1730
10. Németh BC, Patai ÁV, Sahin-Tóth M, et al. Misfolding cationic trypsinogen variant p.L104P causes hereditary pancreatitis. Gut 2016, 66:1727–1728

SIGNIFICANCE OF THIS STUDY

What is already known on this subject?

Loss-of-function mutations in *CPA1* encoding the digestive enzyme carboxypeptidase A1 cause early onset chronic pancreatitis. Cell culture experiments indicate that pathogenic *CPA1* variants induce enzyme misfolding, which results in diminished secretion, intracellular retention and degradation, with consequent endoplasmic reticulum stress.

What are the new findings?

To study the mechanism of action of *CPA1* variants *in vivo*, we generated a novel *CPA1 N256K* knock-in mouse strain, which carries the most frequently occurring human *CPA1* p.N256K mutation in the mouse *Cpa1* gene.

The *CPA1 N256K* mice develop spontaneous and progressive chronic pancreatitis and exhibit signs of endoplasmic reticulum stress in their pancreas.

How might it impact on clinical practice in the foreseeable future?

This is the first mouse model of spontaneous chronic pancreatitis associated with digestive enzyme misfolding and endoplasmic reticulum stress. The model is ideal for testing the effects of various environmental factors (alcohol, smoking, high-fat diet) or pharmaceutical drugs on the onset and progression of the disease.

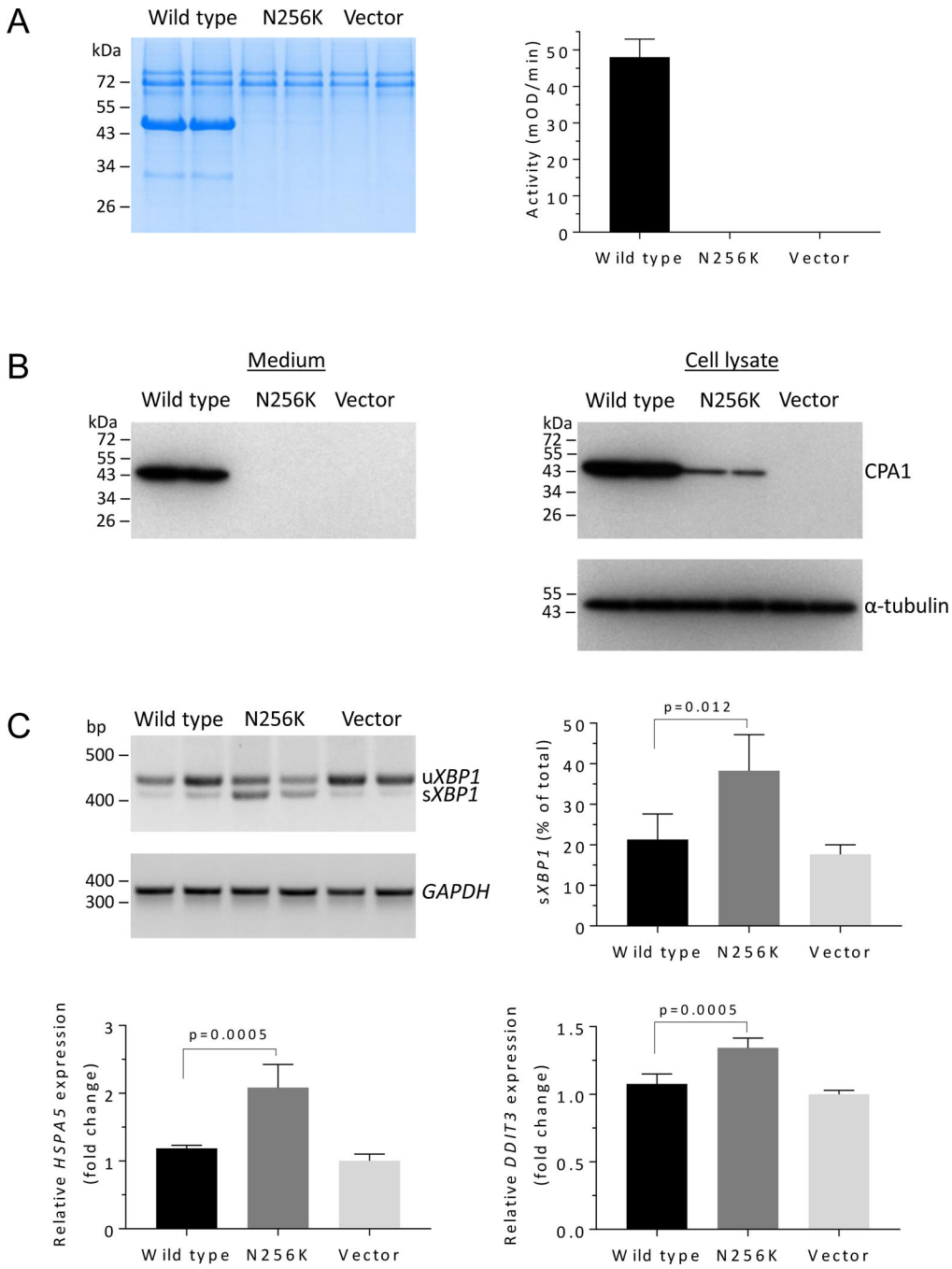

Figure 1.

Effect of the human CPA1 mutation p.N256K on mouse CPA1. HEK 293T cells were transiently transfected with the indicated plasmids and conditioned media and cell lysates were harvested after 48 h. **A**, Secreted levels of CPA1 in the medium were determined by SDS-PAGE and Coomassie Blue staining (left panel) and CPA1 enzyme activity measurements (right panel, mean ± S.D., n=5). **B**, Western blot analysis of CPA1 in the culture medium (left panel) and in cell lysates (right panel) with α-tubulin measured as loading control. **C**, Total RNA prepared from cell lysates was transcribed to cDNA and used

to measure markers of ER stress. Splicing of *XBP1* was assessed by co-amplification of the spliced (s*XBP1*) and unspliced (u*XBP1*) forms followed by agarose gel electrophoresis and ethidium bromide staining. The left panel shows a representative gel with *GAPDH* measured as loading control. The right panel indicates densitometric evaluation of 4 independent experiments (mean ± S.D.). *HSPA5* and *DDIT3* mRNA expression was measured by qPCR and expressed as fold change relative to vector-transfected cells (mean ± S.D., n=4).

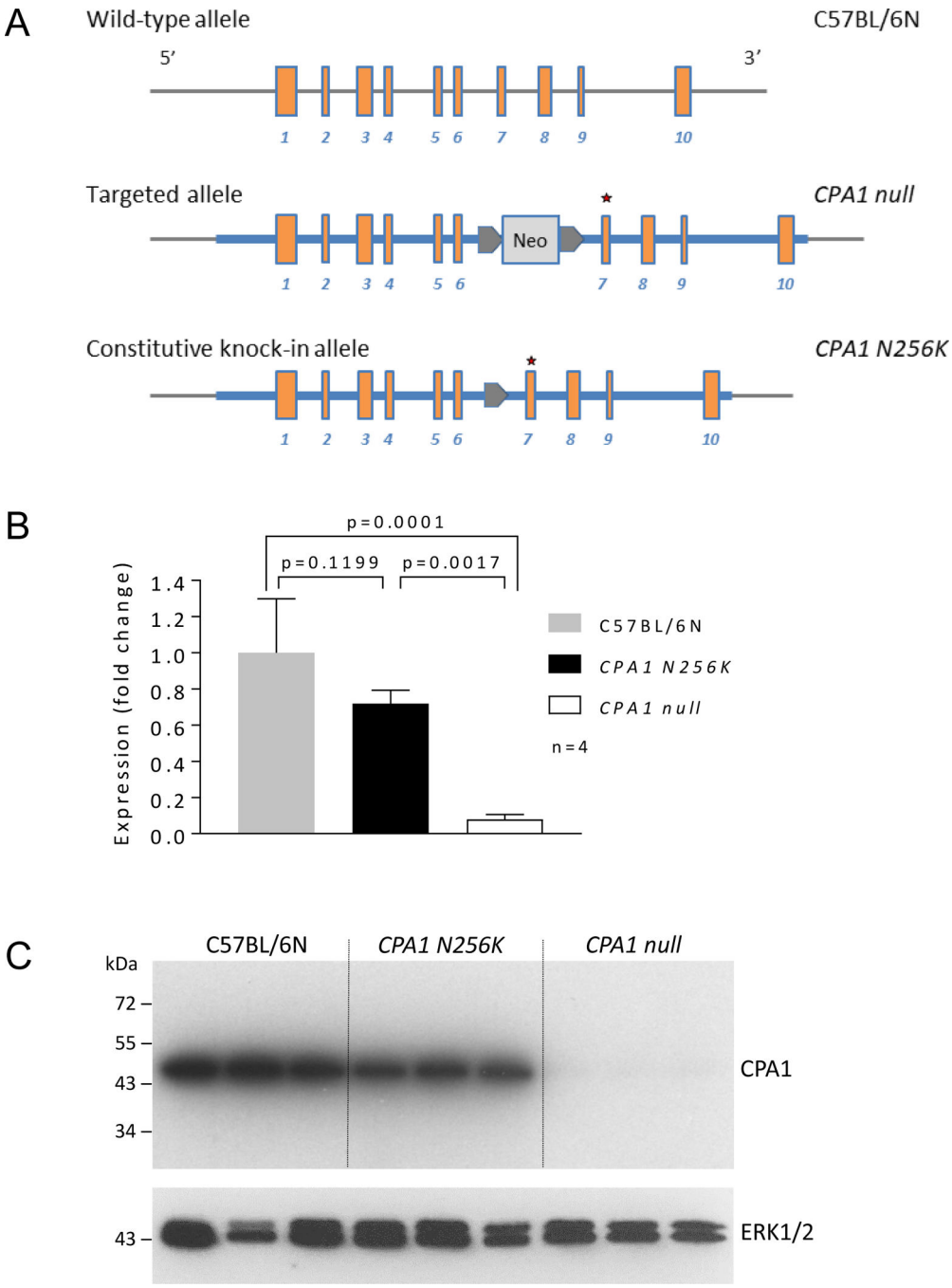

Figure 2.

Generation of *CPA1 N256K* mice and expression of the mutant allele. **A**, The homologous recombination based targeting strategy first yielded an intermediary strain carrying the p.N256K mutation in exon 7 (asterisk) and a neomycin resistance gene (Neo) flanked by loxP sites (gray arrowheads) in intron 6. This strain showed diminished CPA1 expression and was designated as *CPA1 null*. To produce the *CPA1 N256K* mice, the neomycin cassette was removed by breeding the *CPA1 null* mice with a Cre-deleter strain. **B**, *Cpa1* mRNA expression in the pancreas of 1-month-old *CPA1 N256K*, *CPA1 null* and C57BL/6N control

mice. Quantitative PCR was performed on pancreatic cDNA samples and results were expressed as fold change relative to the average of the C57BL/6N results. Mean values with S.D. (n=4) are shown. **C**, Western blot analysis of CPA1 protein expression in the pancreas of 1-month-old *CPA1 N256K*, *CPA1 null* and C57BL/6N control mice. ERK1/2 was measured as loading control.

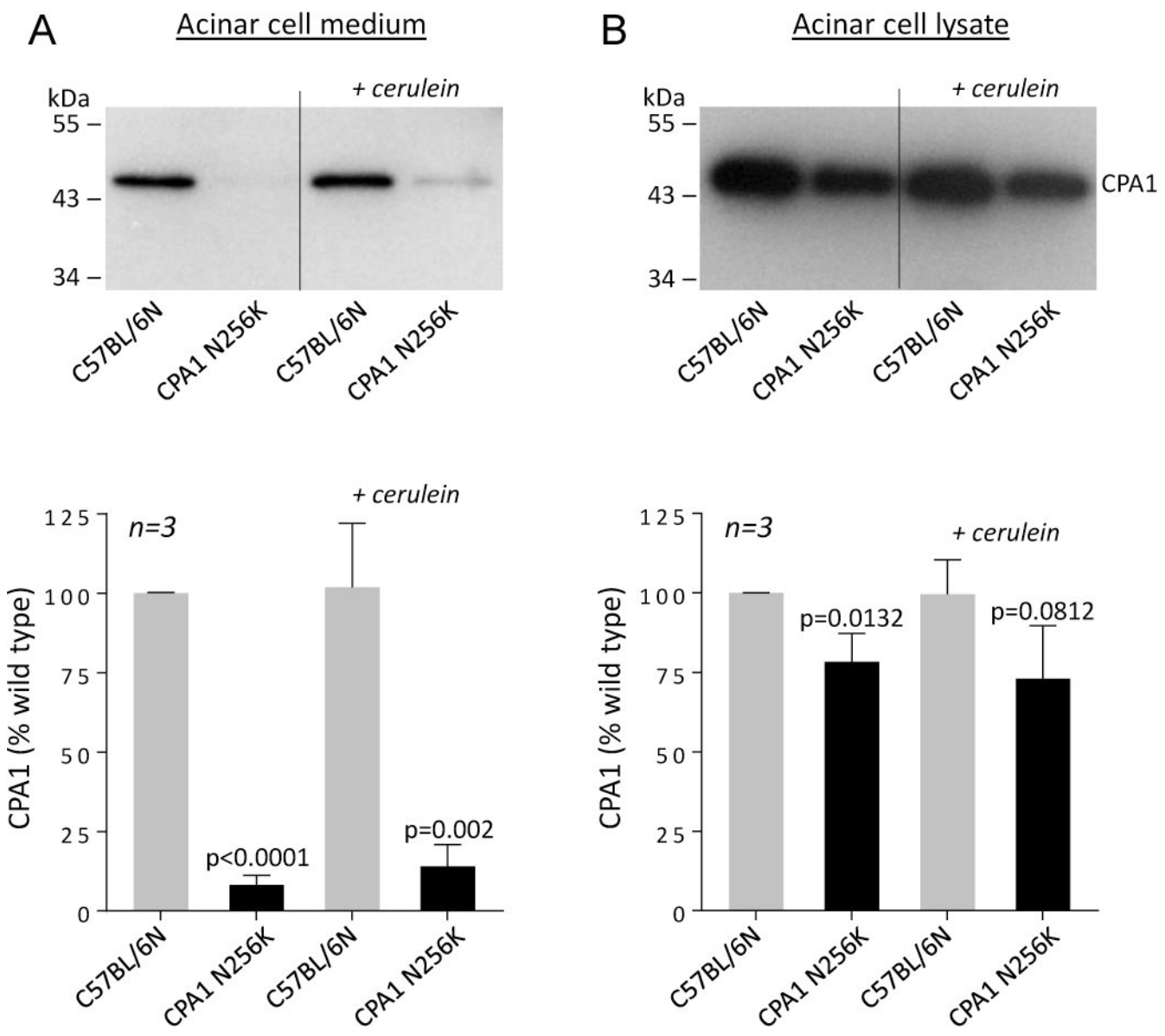

Figure 3.

Spontaneous and cerulein-induced secretion of CPA1 protein from isolated acinar cells of *CPA1 N256K* and C57BL/6N control mice. **A**, CPA1 secretion to the culture medium after 60 min incubation without or with 30 pM cerulein. Note that sample loading was normalized to the amylase content in the medium, which masks the stimulatory effect of cerulein. **B**, CPA1 content in cell lysates after 60 min incubation without or with 30 pM cerulein. Sample loading was normalized to total protein (2 μg). Representative western blots and the results of densitometric analyses from three independent experiments are shown.

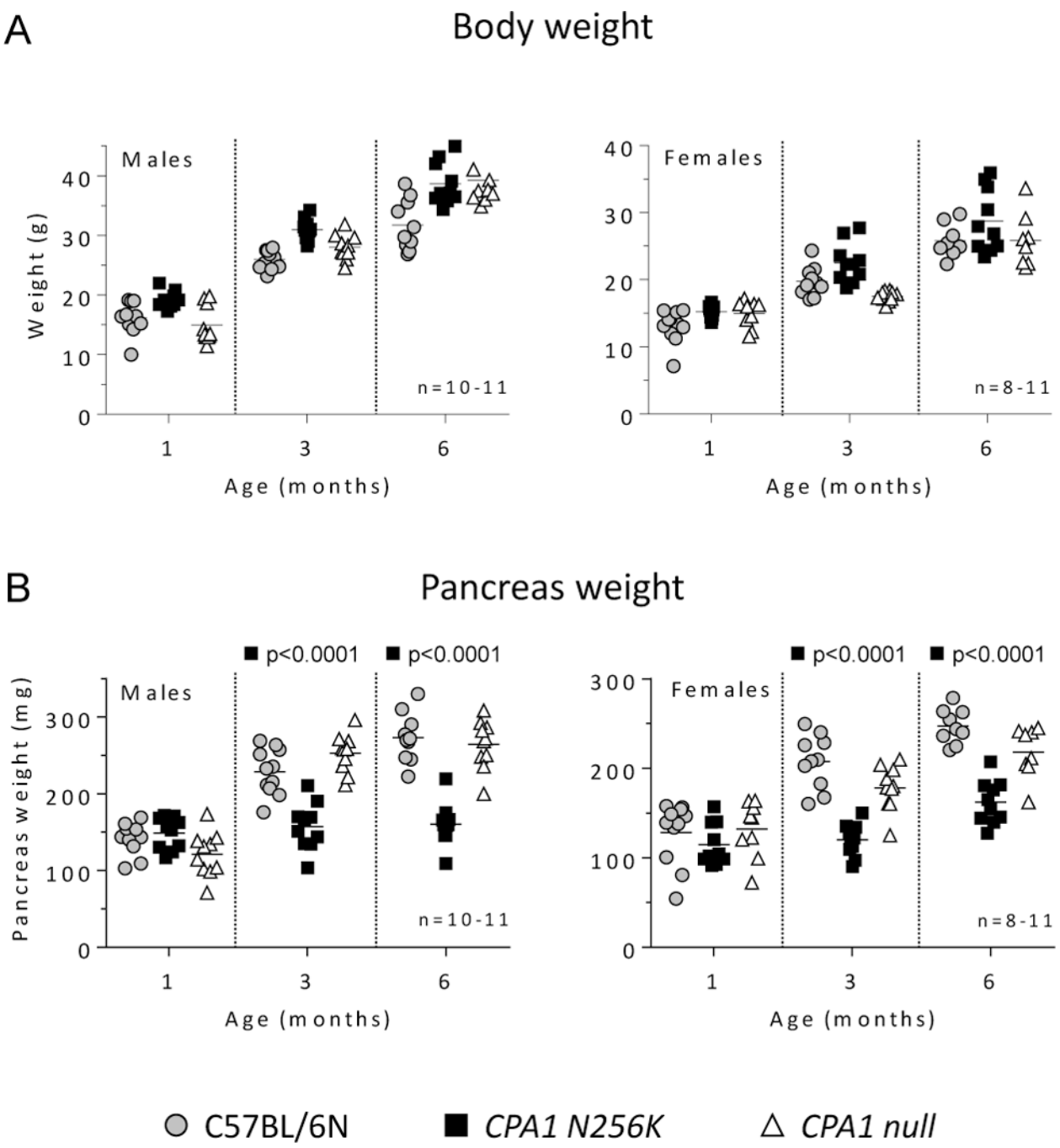

Figure 4.

Body weight and pancreas weight as a function of age in *CPA1 N256K*, *CPA1 null* and C57BL/6N control mice. Individual values with the mean (horizontal bar) are shown. **A**, Body weight. **B**, Pancreas weight. Note that some of the body weight differences in the male group reached statistical significance at 3 months and 6 months. Since these small changes have no obvious biological meaning, we did not indicate p values.

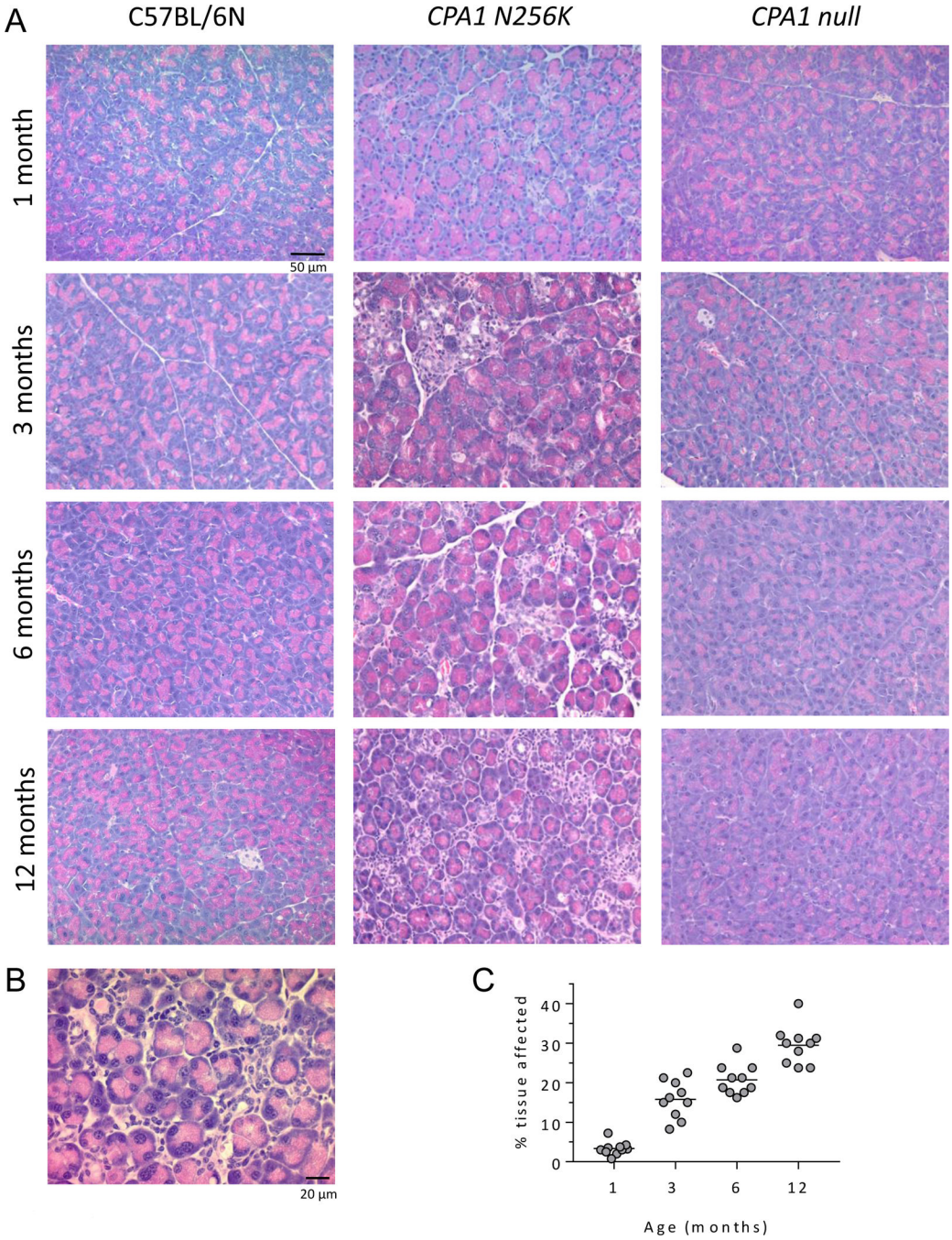

Figure 5.

Pancreas histology as a function of age in *CPA1 N256K*, *CPA1 null* and C57BL/6N control mice. **A**, Hematoxylin-eosin stained pancreas sections. Note the progressive pathology in *CPA1 N256K* mice. **B**, Higher magnification of a pancreas section from a 12-month old *CPA1 N256K* mouse showing the typical morphological changes consisting of loss of acini, inflammatory cell infiltration, pseudotubular complexes and some acinar cell vacuolization. **C**, Quantitation of acinar cell dropout in *CPA1 N256K* mice as a function of age. Individual values with mean (horizontal bar) are shown.

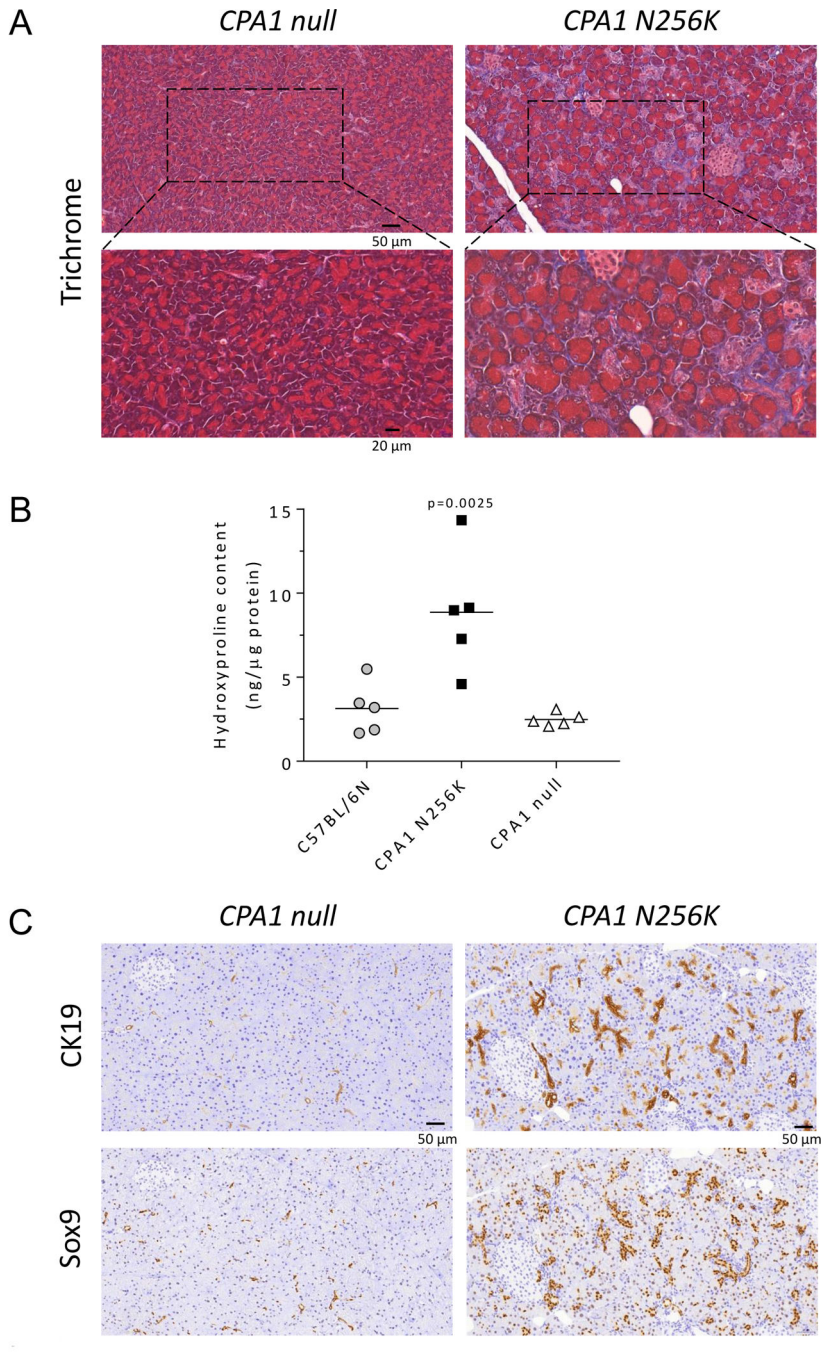

Figure 6.

Fibrosis and acinar-ductal metaplasia in *CPA1 N256K* mice. **A**, Masson's trichrome staining demonstrates widespread fine fibrotic changes (blue color) surrounding acini in *CPA1 N256K* mice but not in *Cpa1 null* mice. **B**, Hydroxyproline content is increased in pancreata from *CPA1 N256K* mice versus *CPA1 null* mice and C57BL/6N controls. Individual values with mean (horizontal bar) are shown. **C**, Immunohistochemistry for cytokeratin 19 (CK19) and Sox9 demonstrates extensive acinar-ductal metaplasia associated with pseudotubular complexes in *CPA1 N256K* mice but not in *Cpa1 null* mice.

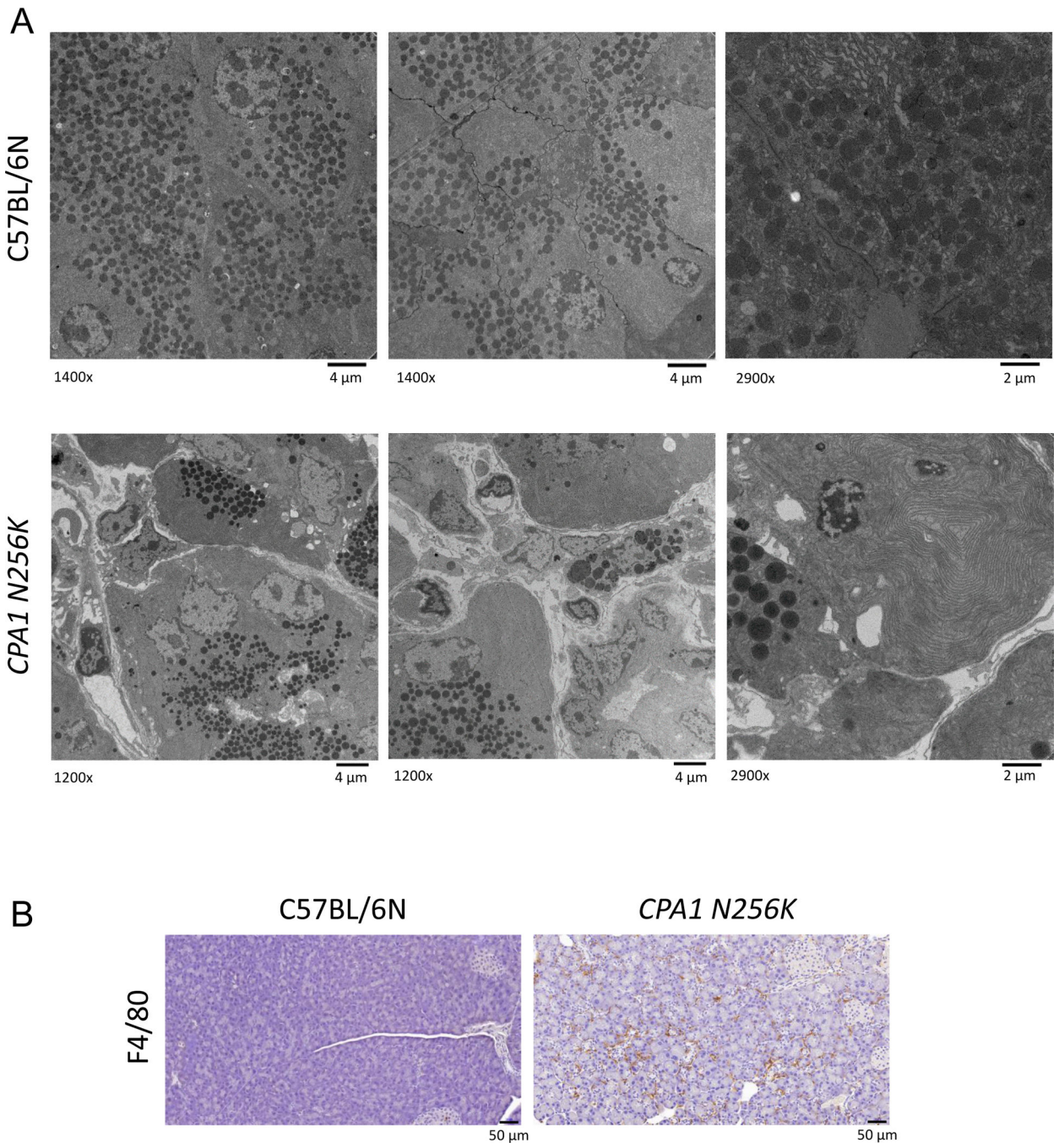

Figure 7.

Ultrastructural changes and macrophage infiltration in *CPA1 N256K* mice. **A**, Electron micrographs of pancreas sections from 4-month-old *CPA1 N256K* mice and C57BL/6N controls. *CPA1 N256K* mice show intact zymogen granules, acinar cell vacuolization, infiltrating macrophages, a pseudotubular complex (middle graph lower right corner), and endoplasmic reticulum whorls (right graph) with no appreciable dilations. Direct magnifications are indicated. **B**, Immunohistochemistry for the F4/80 marker confirms macrophage infiltration in the pancreas of *CPA1 N256K* mice.

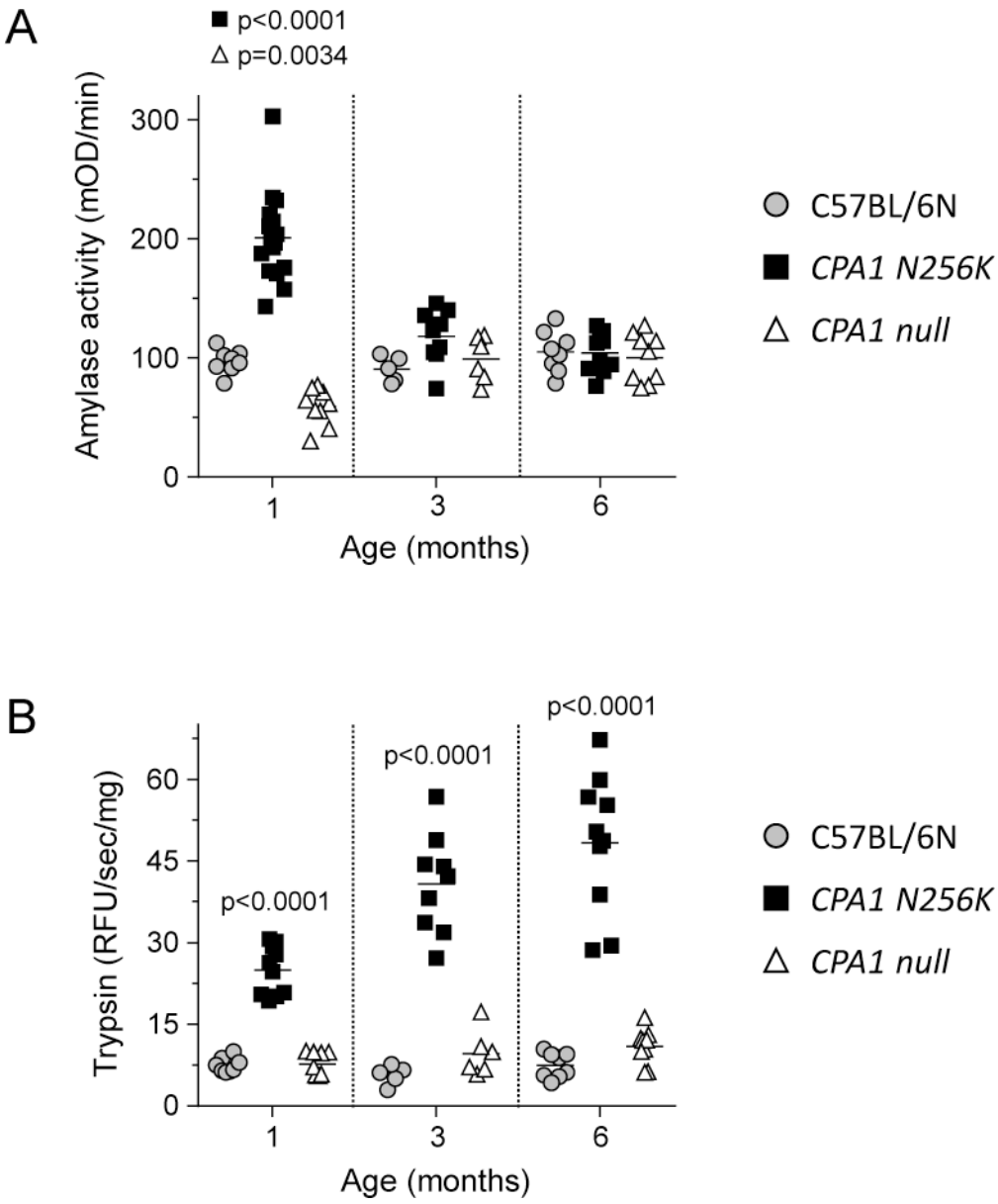

Figure 8.

Plasma amylase (**A**) and intra-pancreatic trypsin activity (**B**) in *CPA1 N256K, CPA1 null* and C57BL/6N control mice at 1, 3 and 6 months of age. Individual values with mean (horizontal bar) are shown.

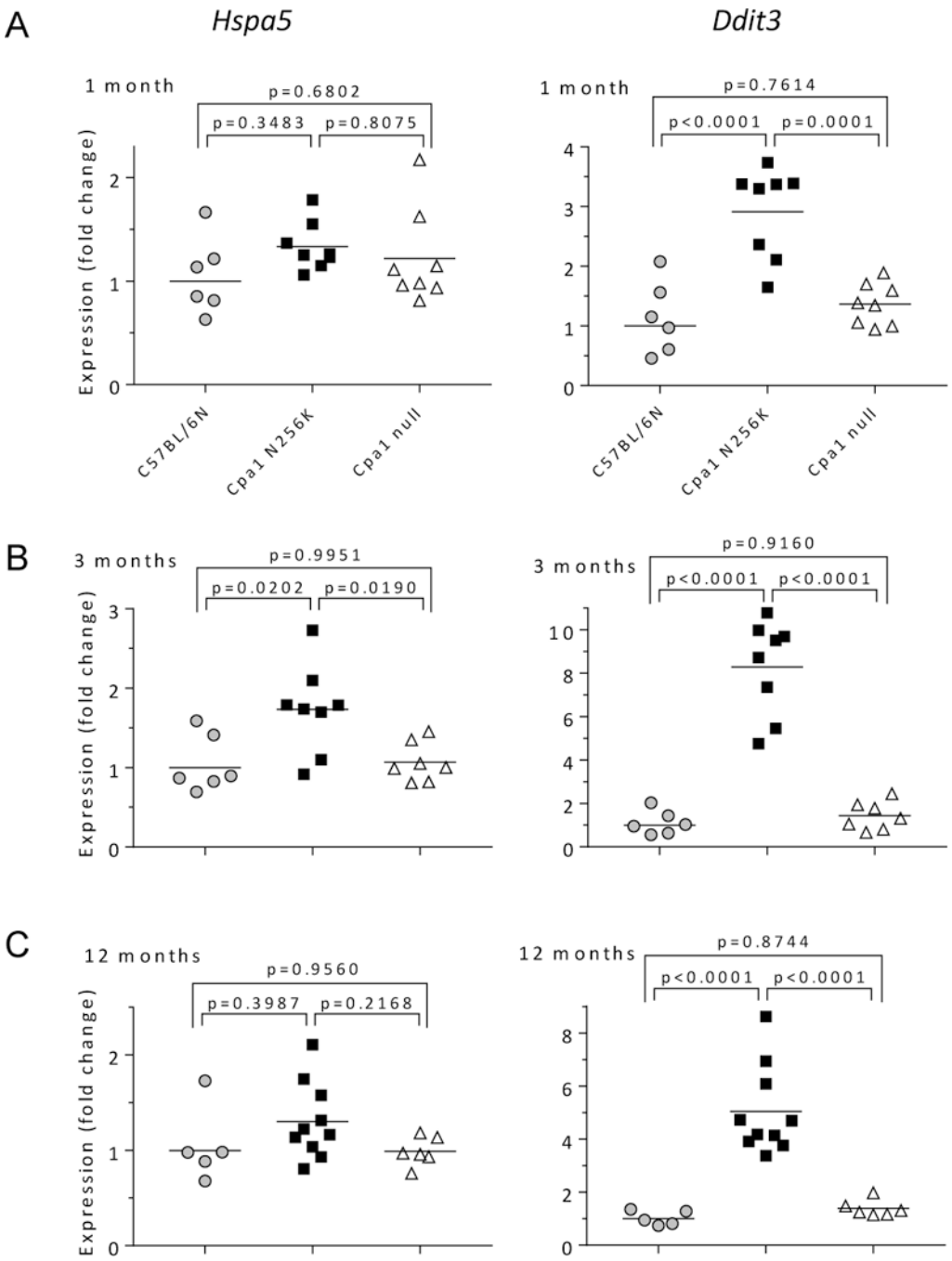

Figure 9.

Expression of endoplasmic reticulum stress markers *Hspa5* and *Ddit3* in *CPA1 N256K*, *CPA1 null* and C57BL/6N control mice at 1 month (**A**), 3 months (**B**) and 12 months (**C**) of age. Quantitative PCR was performed on pancreatic cDNA samples and results were expressed as fold change relative to the average of the C57BL/6N results. Individual values with mean (horizontal bar) are shown.